Nanoparticle Biomarkers

DOI: 10.1002/anie.200902893

$ZrO(HPO_4)_{1-x}(FMN)_x$: Quick and Easy Synthesis of a Nanoscale Luminescent Biomarker**

*Marcus Roming, Heinrich Lünsdorf, Kurt E. J. Dittmar, and Claus Feldmann**

Dedicated to Professor Werner Mader on the occasion of his 60th birthday.

Imaging techniques (such as positron emission tomography, magnetic resonance tomography, X-ray tomography, luminescence imaging, optical coherence tomography, ultrasonic techniques) require new contrasting agents in humans, mice, or rats to visualize whole organisms or single cells.[1] Moreover, new luminescent tags have to be developed for modern light microscopy. Subcellular-ultrastructural analysis with energy-filtered transmission electron microscopy (EFTEM) requires electron-opaque markers for easy detection. To use custom-made nanoparticles as oligofunctional entities, various traits are prerequisite for a general application in life sciences and basic medical research, these include: 1) sufficient biocompatibility; 2) straightforward synthesis; 3) easy detection with standard hardware, and 4) highly specific signals to prevent overlaps with autofluorescence by organs, cells, or organelles. Significant progress has been already made with regard to the above requirements and functions based on luminescent nanoparticles, and is summarized in some recent reviews.[2]

Three classes of luminescent nanoparticles have been identified at present: semiconductor-type quantum dots,[3] metal-doped oxides and fluorides,[4] and organic–inorganic hybrids.[5] Among them, quantum dots (e.g., CdSe@ZnS, InP@ZnS) are most prominent and widely applied, owing to their intense emission, ranging from the blue to the infrared.[6] These materials, however, have inherent drawbacks, such as their sensitivity towards hydrolysis and oxidation, high demands on the crystallinity of the material, and very toxic constituents.[7] Advanced chemical synthesis and strategies for surface protection are prerequisites for obtaining state-of-the-art water-dispersible core–shell structures with precise size control.[8] The size control is essential to establish the underlying quantum size effect and a well-defined emission. Similar requirements—including the crystallinity of the material, core–shell structures, and surface protection—also apply to metal-doped nanoparticles (e.g., $LaPO_4$:Ce,Tb@$LaPO_4$, LaF_3:Eu@LaF_3) to reduce surface-allocated defects and to obtain an intense emission.[9]

Hybrid materials, as an alternative class of luminescent nanoparticles, comprise a nonluminescent inorganic matrix (silica or calcium phosphate), in which a fluorescent organic dye (e.g. phenoxazine, Nile red, rhodamine, indocyanine green, fluorescein) is encapsulated.[10] With a dye concentration of 1 mol% or less, the number of luminescent centers per particle is low, especially, in comparison to the quantum dots. Moreover, the available quantities are limited since these hybrid materials are commonly made by microemulsion techniques.

The aim of our study is to identify a low-cost biocompatible hybrid nanomaterial with intense luminescence. Chemical synthesis should be as easy as possible and potentially provide reliable access to large quantities. The system $ZrO(HPO_4)_{1-x}(FMN)_x$ ($x = 0$–1) and its formal constituents ZrO^{2+}, HPO_4^{2-}, FMN^{2-} (FMN: flavin mononucleotide, a derivative of vitamin B_2, Figure 1)[11] attracted our attention for several reasons: 1) The very low solubility, which facilitates nucleation and growth of nanoparticles;[12] 2) The chemical inertness of zirconium phosphates; 3) All the constituents are known for their biocompatibility (e.g., lethal intake of $ZrCl_4 > 1\ g\,kg^{-1}$);[13] 4) Depending on the chemical composition, the dye concentration can be tuned from very low (< 1 mol%) up to molar amounts. The underlying concept of a luminescent hybrid material that is formally composed of an inorganic cation and an anionic fluorescent dye has not been reported previously.

The poor solubility of the zirconium phosphates, in principle, allows the preparation of nanoparticles by various methods. Aiming at a rapid synthesis that avoids advanced multistage procedures, we have decided to use a forced hydrolysis in water.[14] Based on a formula $ZrO(HPO_4)_{1-x}(FMN)_x$ ($x = 0$–1) a complete exchange of HPO_4^{2-} and FMN^{2-} should be possible, and is indeed observed for the first time for luminescent hybrid materials. To this end, the compound zirconyl flavin mononucleotide (ZrO(FMN)) containing molar amounts of the dye, and the "diluted" version $ZrO(HPO_4)_{0.9}(FMN)_{0.1}$ were selected as representative examples.

[*] M. Roming, Prof. Dr. C. Feldmann
Institut für Anorganische Chemie, Karlsruhe Institute of Technology (KIT)
Engesserstrasse 15, 76131 Karlsruhe (Germany)
Fax: (+49) 721-608-4892
E-mail: claus.feldmann@kit.edu
H. Lünsdorf, K. E. J. Dittmar
Helmholtz-Zentrum für Infektionsforschung GmbH
Braunschweig (Germany)

[**] M.R. and C.F. are grateful to the DFG Center for Functional Nanostructures (CFN) at the Karlsruhe Institute of Technology (KIT) as well as to the Schwerpunktprogramm 1362 "Poröse Metallorganische Gerüstverbindungen" of the Deutsche Forschungsgemeinschaft (DFG) for financial support. H.L. and K.E.J.D. acknowledge I. Kristen for conducting cell embedment and ultrathin sectioning for TEM samples, and Dr. S. Lienenklaus for help on the Xenogen-IVIS system (both at Helmholtz-Zentrum für Infektionsforschung GmbH, Braunschweig).

Supporting information for this article is available on the WWW under http://dx.doi.org/10.1002/anie.200902893.

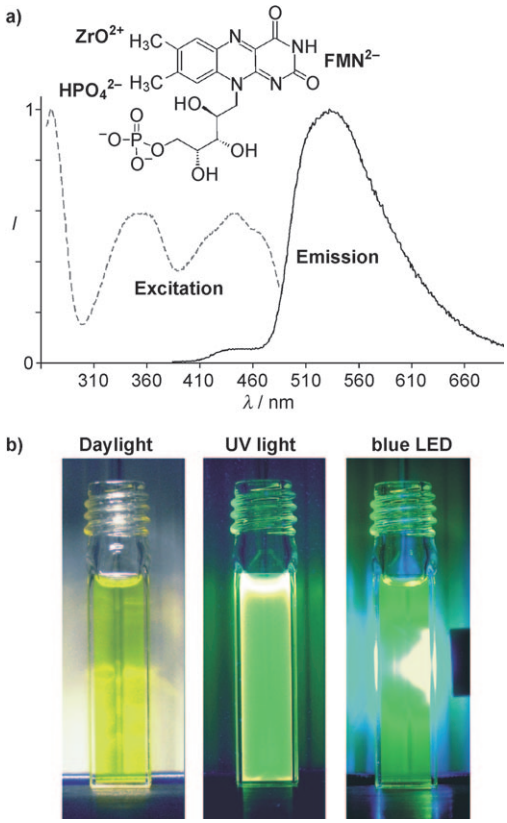

Figure 1. $ZrO(HPO_4)_{1-x}(FMN)_x$ (FMN: flavin mononucleotide) with: a) Its formal constituents as well as excitation and emission spectra; b) Suspensions of as-prepared nanoparticles (1 wt% in ethanol) in daylight, with UV excitation (366 nm), and with blue-LED excitation (380–450 nm).

Both compounds were obtained simply by mixing aqueous solutions of the starting materials and resulted in transparent yellow to orange suspensions, which show bright green emission under ultraviolet (366 nm) as well as under blue light (380–450 nm) excitation (Figure 1). Note that, because of the strong absorption of UV light, only the part of the suspension which is close to the direction of incidence of the incoming light shows full luminescence. In the case of the blue light emitting diode (LED), partial additive color mixing of scattered blue light and green emission is observed, leading to white light. As-prepared suspensions typically contain solid contents of 1% by weight, and turn out to be stable over months. Although the synthesis was performed on the laboratory scale (i.e. in 0.5–1.0 g amounts), straightforward scaling up can be expected because the material's crystallinity or core–shell structures do not need any consideration.

The size and shape of as-prepared $ZrO(HPO_4)_{1-x}(FMN)_x$ was evaluated by dynamic light scattering (DLS), scanning electron microscopy (SEM), and transmission electron microscopy (TEM). DLS analysis of as-prepared nanoparticles in water shows a relatively broad size distribution with a mean hydrodynamic diameter of (39 ± 12) nm (Figure 2). Redispersion in a more surface-active solvent, such as diethylene glycol (DEG), leads to a much narrower size distribution ((32 ± 4) nm). This finding indicates that uniform primary particles are present in principle, but that a certain agglomeration in water occurs. Note that all the particles are still smaller than 100 nm, even in water. Consider also the simplicity of the synthesis and the absence of any common colloidal stabilizer (e.g. long-chained amines or phosphines). By electron microscopy, $ZrO(HPO_4)_{1-x}(FMN)_x$ was observed to have a spherical shape and a mean diameter of 25–40 nm (Figure 2). Finally, the specific surface was measured, based on the Brunauer-Emmett-Teller (BET) method. With a value of 115 $m^2 g^{-1}$, the presence of a nanoscaled compound is again confirmed.

To identify the chemical composition of the title compound, X-ray powder diffraction (XRD) analysis was conducted. However, the nanoparticles turned out to be completely amorphous. Using Fourier-transform infrared spectroscopy (FT-IR) indicated the presence and relative concentration of FMN by comparing $ZrO(HPO_4)_{0.9}(FMN)_{0.1}$ and ZrO(FMN) with $ZrO(HPO_4)$ and $Na(HFMN)\cdot 2H_2O$ as references (see Supporting Information). To investigate dye concentration and chemical composition, energy-dispersive X-ray absorption (EDX), elemental analysis, and thermogravimetry (TG) were conducted. The Zr:P ratio of both compounds was determined by EDX which gave 1:1.2 for the composition $ZrO(HPO_4)_{0.9}(FMN)_{0.1}$ and 1:1.0 for ZrO(FMN). Both values are in agreement with the expected equimolar ratio. Elemental analysis (C/N analysis) revealed C 9.9% and N 2.2% nitrogen by weight (expected C 8.5%, N 2.3%) for $ZrO(HPO_4)_{0.9}(FMN)_{0.1}$ and C 33.6% and N 9.2% nitrogen by weight (expected C 36.3%, N:9.9%) for ZrO(FMN). Thermogravimetry of $ZrO(HPO_4)_{0.9}(FMN)_{0.1}$ showed

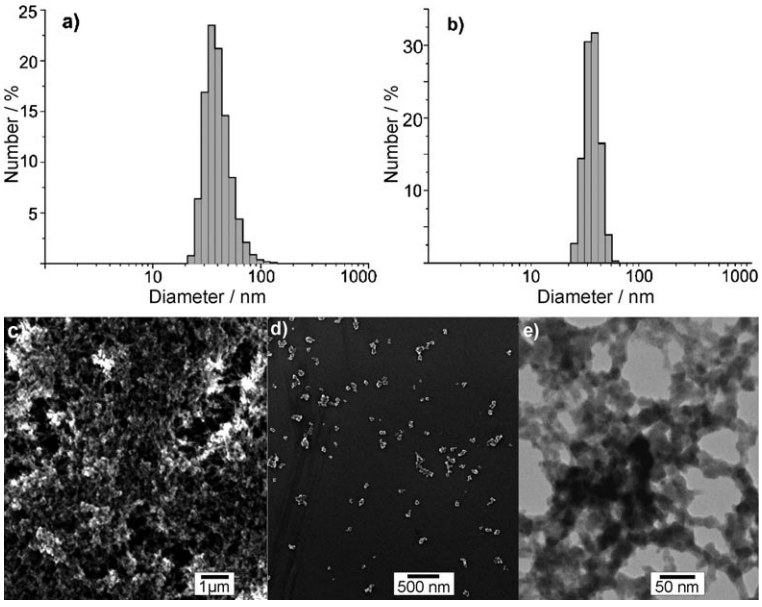

Figure 2. Size and morphology of $ZrO(HPO_4)_{1-x}(FMN)_x$: DLS analysis of as-prepared nanoparticles in water (a) and after redispersion in diethylene glycol (b); Electron microscopy of as-prepared nanoparticles at different magnification including overview SEM (c,d) and energy-filtered TEM zero-loss images (e).

a weight loss of 23% when heated to 700°C. This value—comprising the decomposition of the dye as well as the dehydration of the inorganic matrix—is in accordance with the expected value (22%). ZrO(FMN) showed a weight loss of 61%, which can be directly correlated to the dye decomposition (expected: 64%). The TG remnants of both compounds were identified by XRD, the results being $Zr_3(PO_4)_4$ and minor amounts of ZrO_2 (see Supporting Information).[15] Taking all these analytical data into account, the chemical composition of the amorphous nanoparticles can be reliably deduced to $ZrO(HPO_4)_{0.9}(FMN)_{0.1}$ and ZrO(FMN). Considering the enormous surface and the noncrystallinity of the nanoparticles, however, a certain amount of protonation/hydration (e.g. $Zr(OH)_2(FMN)$) can not be excluded completely. Thus, single-crystal structure analysis would be most preferable to explore the entire structure and bonding situation. Note that detailed structure and composition even of crystalline bulk zirconium phosphates are part of a controversial discussion so that conclusions by analogy are difficult.[15,16]

As expected, the photoluminescence of $ZrO(HPO_4)_{0.9}(FMN)_{0.1}$ and ZrO(FMN) is driven by the dye anion. Accordingly, the nanoparticles can be excited from the UV far into the visible spectrum (250–510 nm), which gives rise to an intense emission with a maximum at 530 nm (Figure 1).[12] Although FMN is very advantageous with regard to biocompatibility, its quantum yield (about 30%)[12] is merely average by comparison to other fluorescent dyes. However, the nanoparticles—especially in the case of ZrO(FMN)—act as a quasi-infinite reservoir owing to the incorporated molar amounts of the dye anion. This huge number of luminescent centers per nanoparticle guarantees an intensive spotlight-type emission as well as a low bleaching.

To evaluate the use of $ZrO(HPO_4)_{1-x}(FMN)_x$ nanoparticles for optical imaging techniques, we have concentrated our studies on living mice and cells. ZrO(FMN) was injected intradermally and intraperitoneally into NMRI (nu/nu) and BALB/C mice. An intense green emission was observed in the resulting wheals (Figure 3a). The blood vessels around the wheals were detected after injection of Cy5-NHS, which reacted with intravascular blood proteins, blood cells, and endothelial cells (Figure 3b). The merged image (Figure 3c) shows the borders of wheals with the vessels (red emission) especially after ethanol injection (ethanol induces hyperemia). The central part of the wheals instead shows intense green emission from the injected nanoparticles. The fluorescence of the ZrO(FMN) nanoparticles in the wheals was stable for several hours and disappeared overnight. The intraperitoneal injection of 100–200 μL of nanoparticles in isotonic phosphate buffer, moreover, did not show any acute toxicity; even after two months, no toxic or allergic effects on the animals were observed.

The biocompatibility of $ZrO(HPO_4)_{1-x}(FMN)_x$ nanoparticles was further investigated with mammalian cells, which respond to toxic substances and show a high uptake rate of nanoparticles (i.e., murine bone-marrow-derived macrophages, immature human dendritic cells). Both cell types took up the nanoparticles without showing any toxic effect, such as blebbing or cell death by apoptosis or necrosis. The nanoparticles colocalized with vesicles of the lysosomal compartment stained with lysotracker (Figure 3d–f). They did not colocalize with mitochondria and nuclei. The total emission spectrum measured over all stained cellular compartments confirmed the colocalization (Figure 3g). SEM and EF-TEM verified the results of light microscopy and show the murine macrophages attached to a plastic surface (Figure 4a–e). The fixed macrophages were cut "en face" in parallel sections. In the case of untreated macrophages, the nucleus and cytoplasm—crowded with electron-translucent vesicles—are clearly visible (Figure 4b,d). In contrast, the cytoplasm of nanoparticle-treated macrophages is enriched with electron-opaque vesicles showing a characteristic dark, granular structure (Figure 4c,e). Accordingly, the nanoparticles are exclusively localized in vesicles. Parallel electron-energy loss (PEEL) spectra of nanoparticle-containing vesicles and of suitable reference materials (i.e., ZrO(FMN) as

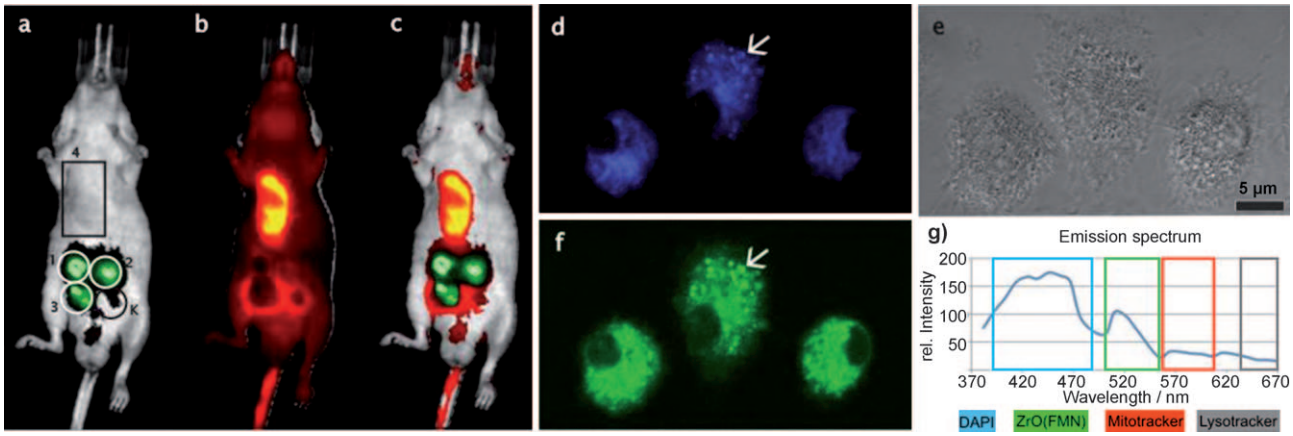

Figure 3. In vivo imaging of $ZrO(HPO_4)_{1-x}(FMN)_x$ nanoparticles in whole organisms and cells: a)–c) Luminescence after intradermal injection into NMRI mice with a) ZrO(FMN) nanoparticles in 1) HEPES-buffer, 2) water, 3) ethanol as well as 4) Cy5-NHS intravescular vessel stain, K = control buffer; b) Red fluorescence of Cy5-NHS; c) Merged images of (a) + (b); d)–f) Cellular uptake of ZrO(FMN) in living murine macrophages with d) vesicles and lysosomes stain by lysotracker; e) DIC image; f) Colocalization of vesicles with luminescent nanoparticles; g) Emission spectrum of four-color stain macrophages. DAPI = 4′,6-diamidino-2-phenylindol.

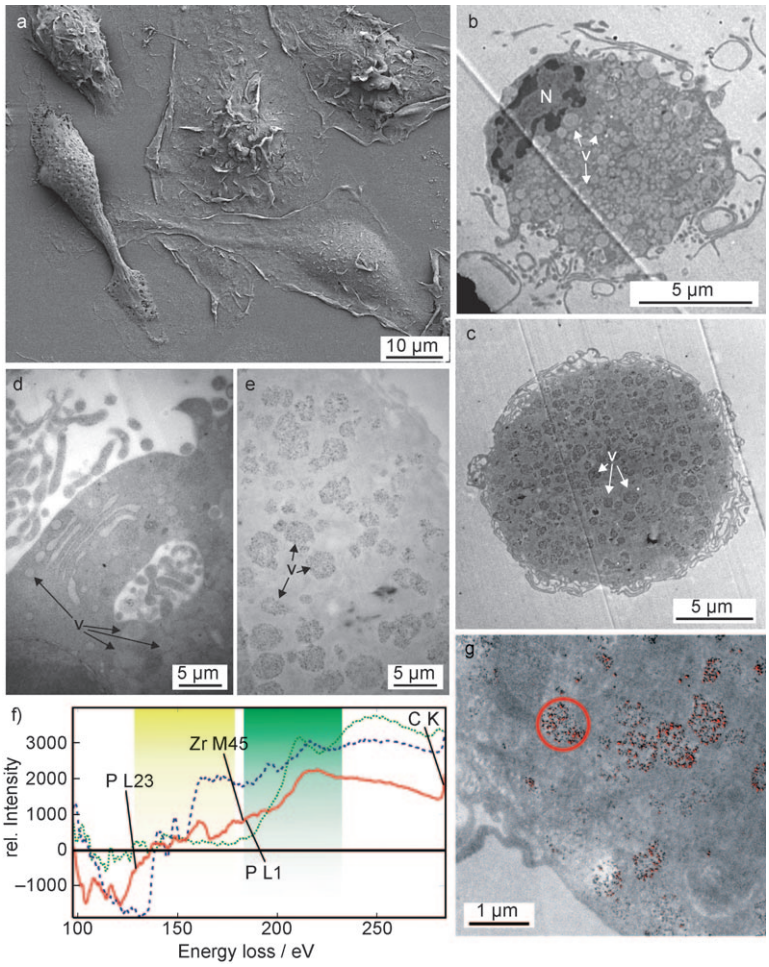

Figure 4. Ultrastructural and elemental analysis of $ZrO(HPO_4)_{1-x}(FMN)_x$-treated macrophages: a) Survey of confluently growing macrophages; b),d) Low-/high-resolution images of untreated macrophages (N: nucleus, V: cytoplasm with vesicles); c),e) Low-/high-resolution images of nanoparticle-treated macrophages; f) WR-PEEL spectra of: nanoparticle-filled vesicle (red line, measured vesicle indicated by red circle in (g)), ZrO(FMN) nanoparticles (blue line), elemental Zr as a reference (green line) as well as ionization onsets P-L23 (yellow box) and Zr-M45 (green box) with ELNES fingerprints; g) Vesicles overlaid with Zr-M45 elemental map indicating ZrO(FMN) nanoparticles as red dots.

such, elemental zirconium, ionization onsets of P-L23 and Zr-M45) indicate the presence of Zr and P in the nanoparticles (Figure 4 f). Macrophages incubated without nanoparticles do not show such structures (negative control). Finally, the ZrO(FMN) nanoparticles become precisely visible if the vesicles were overlaid with an Zr-M45 elemental map (Figure 4 f).

$ZrO(HPO_4)_{1-x}(FMN)_x$ nanoparticles appear to be suitable tools for staining viable structures in whole organisms. To introduce specific targeting in organisms, organs, or cells—that is, to couple specific antibodies, ligands, lectins, or receptor molecules—all the established techniques to functionalize the surface of semiconductor quantum dots and to attach specific linkers can now be applied.[2–9]

In addition to $ZrO(HPO_4)_{1-x}(FMN)_x$ showing green emission, the concept of dye-modified zirconium phosphates (DMZPs) has been extended in a preliminary study to other dye anions and different emission colors. When umbelliferon phosphate $(UFP)^{2-}$ was introduced, noncrystalline nanoparticles with an approximated composition "ZrO(UFP)" were obtained, exhibiting blue emission under 366 nm excitation (Figure 5). In fact, emission is relatively weak in this case. A much brighter luminescence occurs if nonbound umbelliferon is set free in the presence of phosphatase. This change from weak to very strong emission can be of great relevance, since the effect can be directly correlated to metabolic activity, for example, ATP consumption. A similar effect occurs in the case of $ZrO(HPO_4)_{1-x}(FMN)_x$, whose emission can be turned on and off reversibly (Figure 5). This is caused by reduction, such as in the presence of $[S_2O_4]^{2-}$, or oxidation, such as in the presence of O_2, of the dye, and might again allow a direct observation of metabolic processes (e.g. in the presence of NADH or NAD^+). A correlation of metabolic processes and optical switching of luminescent markers very recently attracted great interest.[17] Finally, red emission of DMZPs has been observed under blue-light excitation with porphyrinamidophosphonate $(PAP)^{8-}$ as the dye anion and an approximated composition "$Zr_4O_4(PAP)$" (Figure 5). As in the case of $ZrO(HPO_4)_{1-x}(FMN)_x$, "ZrO(UFP)" and "$Zr_4O_4(PAP)$" require a much more detailed elaboration of structure and properties as part of future studies. Nevertheless, both compounds demonstrate the practicability of DMZPs as a novel class of luminescent nanoparticles on a broader scope.

In summary, the compound $ZrO(HPO_4)_{1-x}(FMN)_x$ is introduced as a novel luminescent material and verified with the composition $ZrO(HPO_4)_{0.9}(FMN)_{0.1}$ and ZrO(FMN). The material has several important features, including a quick and easy water-based synthesis, potentially low costs of production, a high biocompatibility, and a variable concentration of the incorporated dye, which allows for quasi-infinite number of luminescent centers. Typical key issues for quantum dots as well as metal-doped nanoparticles, such as high-temperature crystallization and core–shell type surface conditioning, do not need any consideration. Taking all these aspects together, $ZrO(HPO_4)_{1-x}(FMN)_x$ might be a promising alternative to existing luminescent nanomaterials. Its use as a luminescent biomarker and its biocompatibility have been successfully tested as a proof of the concept in living mice and cells. Finally, the concept of DMZPs has been extended to red and blue emission as well as to luminescent switching.

Experimental Section

$ZrO(HPO_4)_{0.9}(FMN)_{0.1}$ was prepared by admixing a solution of $ZrOCl_2{\cdot}8H_2O$ (40 mg; Aldrich, Steinheim, >99%) in methanol (0.5 mL) to a solution of sodium riboflavin-5′-monophosphate dihydrate (Na(HFMN), 10 mg; Fluka, Buchs, 85%) and crystalline

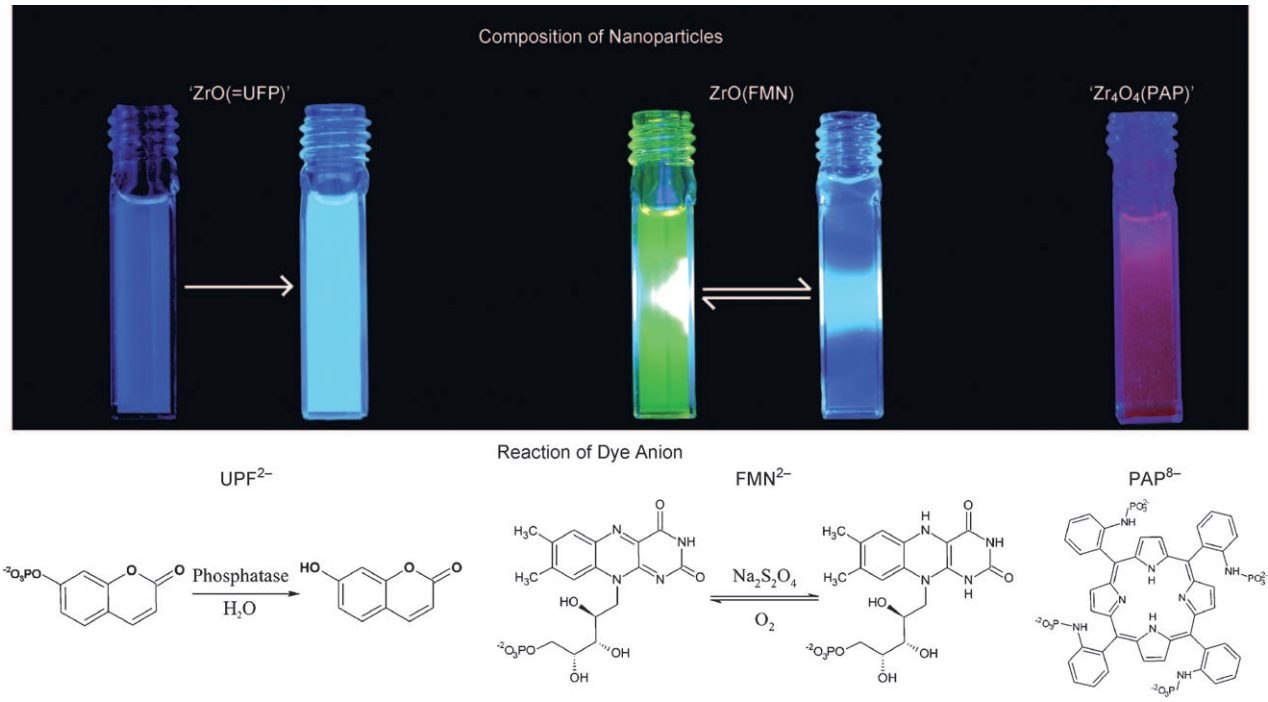

Figure 5. DMZPs with alternative emission color and luminescent switching: Combining the formal constituents ZrO^{2+} and umbelliferonphosphate UFP^{2-} or porphyrinamidophosphonate PAP^{8-} as dye anions resulted in nanoparticles exhibiting blue and red emission ($\lambda_{excitation} = 366$ nm). Luminescent switching is possible by addition of phosphatase in the case of "ZrO(UFP)" and by reduction/oxidation in the case of ZrO(FMN) (ZrO(FMN) excited with blue LED).

phosphoric acid (20 mg; Sigma–Aldrich, Steinheim, 85%) in H_2O (45 mL) at 70°C. Admixing was performed with vigorous stirring. After 2 min of stirring the orange solid product was separated by centrifuging (15 min at 25000 r.p.m.). The nanoparticles were twice re-suspended in and centrifuged from H_2O to remove all remaining salts. Finally, stable suspensions were obtained by re-suspending the resulting nanoparticles in water, followed by a removal of a minor amount of agglomerates by centrifuging (2 min, 4000 r.p.m.). A stable suspension was also established by direct re-dispersion in diethylene glycol (DEG), which did not need any removal of agglomerates. Powder samples were obtained by centrifugation of suspensions in ethanol, followed by drying of the solid residue for 1 h at 100°C in a drying oven to remove surface-bound solvents (i.e. water, ethanol).

ZrO(FMN): Zirconyl flavinmononucleotide was prepared similarly to $ZrO(HPO_4)_{0.9}(FMN)_{0.1}$, however, the compound was obtained by admixing a solution of $ZrOCl_2 \cdot 8H_2O$ (100 mg; Aldrich, Steinheim, > 99%) in H_2O (5 mL) to a solution of sodium riboflavin-5′-monophosphate dihydrate (Na(HFMN), 480 mg; Fluka, Buchs, 85%) in H_2O (50 mL).

Further information regarding chemical analysis and biological testing can be found in the Supporting Information.

Received: May 29, 2009
Revised: September 18, 2009
Published online: December 22, 2009

Keywords: biomarker · imaging agents · luminescence · nanomaterials · organic–inorganic hybrid composites

[1] J. G. Fujimoto, D. Farkas, *Biomedical Optical Imaging*, Oxford University Press, Oxford, **2009**.
[2] a) H. Hang, D. Yee, C. Wang, *Nanomedicine* **2008**, *3*, 83–91; b) R. C. Somers, M. G. Bawendi, D. G. Nocera, *Chem. Soc. Rev.* **2007**, *36*, 579–591; c) X. Michalet, F. F. Pinaud, L. A. Bentolila, J. M. Tsay, S. Doose, J. J. Li, G. Sundaresan, A. M. Wu, S. S. Gambhir, S. Weiss, *Science* **2005**, *307*, 538–544.
[3] a) B. Nitzsche, F. Ruhnow, S. Diez, *Nat. Nanotechnol.* **2008**, *3*, 552–556; b) S. J. Clarke, C. A. Hollmann, Z. Zhang, D. Suffern, S. E. Bradforth, N. M. Dimitrijevic, W. G. Minarik, J. L. Nadeau, *Nat. Mater.* **2006**, *5*, 409–417; c) M. K. So, C. Xu, A. M. Loening, S. S. Gambhir, J. Rao, *Nat. Biotechnol.* **2006**, *24*, 339–343.
[4] X. F. Yu, L. D. Chen, M. Li, M. Y. Xie, L. Zhou, Y. Li, Q. Q. Wang, *Adv. Mater.* **2008**, *20*, 4118–4123.
[5] C. Sanchez, B. Lebeau, F. Chaput, J. P. Boilot, *Adv. Mater.* **2003**, *15*, 1969–1994.
[6] a) A. M. Smith, S. Dave, S. Nie, L. True, X. Gao, *Expert Rev. Mol. Diagn.* **2006**, *6*, 231–244; b) Z. Liu, A. Kumbhar, D. Xu, J. Zhang, Z. Sun, J. Fang, *Angew. Chem.* **2008**, *120*, 3596–3598; *Angew. Chem. Int. Ed.* **2008**, *47*, 3540–3542.
[7] a) Y. Su, Y. He, H. Lu, L. Sai, Q. Li, W. Li, L. Wang, P. Shen, Q. Huang, C. Fan, *Biomaterials* **2008**, *30*, 19–25; b) J. Curtis, M. Greenberg, J. Kester, S. Phillips, G. Krieger, *Toxicol. Rev.* **2006**, *25*, 245–260.
[8] a) J. S. Steckel, J. P. Zimmer, S. Coe-Sullivan, N. E. Scott, V. Bulovic, M. G. Bawendi, *Angew. Chem.* **2004**, *116*, 2206–2210; *Angew. Chem. Int. Ed.* **2004**, *43*, 2154–2158; b) X. L. Peng, L. Manna, W. Yang, J. Wickham, E. Scher, A. Kadavanich, A. P. Alivisatos, *Nature* **2000**, *404*, 59–61.
[9] a) F. Meiser, C. Cortez, F. Caruso, *Angew. Chem.* **2004**, *116*, 6080–6083; *Angew. Chem. Int. Ed.* **2004**, *43*, 5954–5957; b) J. W. Stouwdam, F. C. J. M. van Veggel, *Langmuir* **2004**, *20*, 11763–11771.
[10] a) I. Sokolov, S. Naik, *Small* **2008**, *4*, 934–939; b) T. T. Morgan, H. S. Muddana, E. I. Altinoglu, S. M. Rouse, T. Tabakivic, T. Tabouillot, T. J. Russin, S. S. Shanmugavelandy, P. J. Butler, P. C. Eklund, J. K. Yun, M. Kester, J. H. Adair, *Nano Lett.* **2008**, *8*, 4108–4115; c) H. Ow, D. R. Larson, M. Srivastava, B. A. Baird, W. W. Webb, U. Wiesner, *Nano Lett.* **2005**, *5*, 113–117.

[11] H. Du, R. A. Fuh, J. Li, A. Corkan, J. S. Lindsey, *Photochem. Photobiol.* **1998**, *68*, 141 – 142.
[12] A. Clearfield, R. H. Blessing, J. A. Stynes, *J. Inorg. Nucl. Chem.* **1968**, *30*, 2249 – 2258.
[13] S. Ghosh, A. Sharma, G. Talukder, *Biol. Trace Elem. Res.* **1992**, *35*, 247 – 271.
[14] E. Matijevic, *Chem. Mater.* **1993**, *5*, 412 – 426.
[15] a) J. M. Troup, A. Clearfield, *Inorg. Chem.* **1977**, *16*, 3311 – 3314; b) J. Alamo, R. Roy, *J. Am. Ceram. Soc.* **1984**, *67*, C80 – C82; c) V. I. Petkov, E. A. Asabina, K. V. Kiryanov, A. V. Markin, N. N. Smirnova, D. B. Kitaev, A. M. Kovalsky, *J. Chem. Thermodyn.* **2005**, *37*, 467 – 476; d) A. Orlova, S. G. Samoilov, G. N. Kazantsev, V. Y. Volgutov, D. M. Bykov, A. V. Golubev, E. Y. Borovikova, *Crystallogr. Rep.* **2009**, *54*, 431 – 438.
[16] a) P. H. Mutin, G. Guerrero, A. Viaux, *C. R. Chim.* **2003**, *6*, 1153 – 1164; b) E. Brunet, M. Alonso, C. Cerro, O. Juanes, J. C. Rodriguez-Ubis, Á. E. Kaifer, *Adv. Funct. Mater.* **2007**, *17*, 1603 – 1610.
[17] a) D. Lee, S. Khaja, J. C. Velasquez-Castano, M. Dasari, C. Sun, J. Petros, W. R. Taylor, N. Murthy, *Nat. Mater.* **2007**, *6*, 765 – 769; b) M. Andresen, A. C. Stiel, J. Folling, D. Wenzel, A. Schonle, A. Egner, C. Eggeling, S. W. Hell, S. Jakobs, *Nat. Biotechnol.* **2008**, *26*, 1035 – 1040; c) W. Wu, A. D. Q. Li, *Nanomedicine* **2007**, *2*, 523 – 531.

